Radiative and Relativistic Effects in the Decay of Highly Excited States in Helium

Thomas Ward Gorczyca,[1,*] Jan-Erik Rubensson,[2] Conny Såthe,[2] Magnus Ström,[2] Marcus Agåker,[2]
Dajun Ding,[3] Stefano Stranges,[4] Robert Richter,[5] and Michele Alagia[6]

[1]*Department of Physics, Western Michigan University, Kalamazoo, Michigan 49008-5151*
[2]*Physics Department, Box 530, S-751 21 Uppsala, Sweden*
[3]*Institute of Atomic and Molecular Physics and State Key Lab of Superhard Materials, Jilin University, Changchun 130023, China*
[4]*Dipartimento di Chimica, Universitá di Roma La Sapienza e Unitá INFM, P. le A. Moro 5, I-00185 Rome, Italy*
[5]*Sincrotrone Trieste, I-340 12 Trieste, Italy*
[6]*INFM-TASC, Padriciano, I-340 12 Trieste, Italy*

(Received 25 February 2000)

A recent experimental study [J.-E. Rubensson *et al.,* Phys. Rev. Lett. **83**, 947 (1999)] measured a significant fluorescence yield of the He($2lnl'$) photoexcited resonances, showing major qualitative differences from nonrelativistic predictions. We present a further theoretical study of these states, and perform R-matrix multichannel quantum defect theory calculations to extract fluorescence and ionization cross sections. These theoretical results are in excellent agreement with newer, higher-resolution measurements. Radiative and spin-orbit effects are quantified and shown to play an important role in the overall characterization of highly excited states.

PACS numbers: 31.50.+w, 32.80.–t, 32.80.Fb, 32.80.Rm

The doubly excited $2lnl'$ photoionization spectrum of helium has been studied extensively over the past three and a half decades, beginning with the pioneering experimental work of Madden and Codling [1] and the corresponding theoretical work of Cooper, Fano, and Prats [2]. While enormous advances in both experimental and theoretical capabilities have led to a detailed understanding of these states [3–5], apparently it had never been necessary to include higher-order effects in their characterization, such as alternate radiative decay channels or relativistic interactions.

In a recent experimental study [6], it was found that the radiative decay of photoexcited He($2lnl'$) states, first observed by Odling-Smee *et al.* [7], has an important influence on the photoionization spectrum. It was also found that the standard description of the high-n members, modified to include radiative effects, still failed to predict the behavior in the near-threshold fluorescence yield.

In this Letter, we reinvestigate the near-threshold photofluorescence behavior by carrying out detailed numerical calculations within an R-matrix multichannel quantum defect theory (MQDT) method. We demonstrate that the inclusion of spin-orbit and radiative effects is essential for reproducing the spectral behavior found in Ref. [6]. Furthermore, we find remarkable agreement with new highly resolved FY data, measured in a recently designed experimental setup. We first describe the theoretical method in some detail, give an intuitive explanation of the spectral behavior, make a brief presentation of the new experiment, compare theoretical and experimental fluorescence results, and finally discuss the implications for the autoionization spectrum.

The theoretical methodology begins with an LS R-matrix calculation [8] including the $n = 1$–5 physical states of He^+ and additional $\overline{n} = 6$ pseudoorbitals optimized on the He($1s^2$) ground state, similar to earlier He pseudostate work [9]. Resulting scattering quantities from this 23 channel calculation are then projected onto the open $1s\epsilon p$ and closed $\{2snp, 2pns, 2pnd\}$ channels. Following MQDT methods [10,11], the inner-region, unphysical scattering, and dipole matrices, both slowly varying functions of energy, are partitioned into open and closed channels,

$$\mathbf{S} = \begin{pmatrix} \mathbf{S}_{oo} & \mathbf{S}_{oc} \\ \mathbf{S}_{co} & \mathbf{S}_{cc} \end{pmatrix}, \qquad \mathbf{d} = \begin{pmatrix} \mathbf{d}_o \\ \mathbf{d}_c \end{pmatrix}, \tag{1}$$

and then projected onto the *physical* scattering and dipole matrices (the $1s\epsilon p$ subspace) by keeping only linear combinations of channels that have exponentially decaying behavior for the closed channel wave functions,

$$\begin{aligned} \mathbf{S}^{\text{phys}} &= \mathbf{S}\begin{pmatrix} \mathbf{1}_{oo} \\ (\mathbf{S}_{cc} - e^{-i2\pi\nu})^{-1}\mathbf{S}_{co} \end{pmatrix}, \\ \mathbf{d}^{\text{phys}} &= [\mathbf{1}_{oo} \quad \mathbf{S}_{oc}(\mathbf{S}_{cc} - e^{-i2\pi\nu})^{-1}]\mathbf{d}\,, \end{aligned} \tag{2}$$

and from the physical dipole matrix, the photoionization cross section is computed as

$$\sigma^{\text{ion}} = \frac{4\pi^2\omega}{3c}\,\mathbf{d}^{\text{phys},\dagger}\mathbf{d}^{\text{phys}}. \tag{3}$$

The diagonal matrix ν, which contains the closed-channel effective quantum numbers defined via $E = E_2 - \frac{1}{2\nu^2}$, plays an important role in the present study, since it counts the nodes in the various closed-channel orbitals. Equivalently, it analytically parametrizes the matching condition between the inner-region R-matrix and outer-region physical solutions given in Eq. (2), allowing a simple modification to the outer-region orbital behavior

 0031-9007/00/85(6)/1202(4)$15.00

via a change in ν. In order to introduce radiative and spin-orbit effects, such a change is required on the physical grounds that the closed-channel nl orbitals, describing the valence electron far away from the atom, propagate in potentials that are affected by the $2p \rightarrow 1s$ radiative decay and the $2p_{1/2} - 2p_{3/2}$ spin-orbit splitting. These additional potentials cause differences in the nodal behaviors of higher-n (more diffuse) orbitals, leading to a breakdown of nonradiative LS-coupling predictions.

At lower n, where radiative and spin-orbit effects can be neglected, there is a threefold degeneracy of the closed channel energies ($E_2 = 1.5$ a.u. relative to the $1s$ state), and ν is simply a multiple of the unit matrix. We can then rotate the closed channels to a diagonal form

$$\mathbf{O}^{\mathrm{T}}\mathbf{S}_{cc}\mathbf{O} = e^{-\pi\tilde{\Gamma}_A + i2\pi\mu_A}, \qquad A = -1, 0, +1. \quad (4)$$

The photoionization cross section can thus be parametrized by three noninteracting series of Fano profiles, with energy positions $E_{A,n} = E_2 - \frac{1}{2(n-\mu_A)^2}$, autoionization widths $\Gamma^a_{A,n} = \frac{\tilde{\Gamma}_A}{(n-\mu_A)^3}$, and Fano q parameters that are somewhat more complicated MQDT functions. Qualitatively, these rotated series were characterized by Cooper, Fano, and Prats [2] as the combinations $2snp \pm 2pns$ and $2pnd$ for $A = \pm 1$ and $A = 0$, respectively, with the important property that the $A = +1$ series has a much larger oscillator strength and autoionization width than the other two series. Quantitatively, the actual mixings and resonance parameters are more complicated [3] and are energy dependent in general [5,12].

At higher n, the $2pnl \rightarrow 1snl + \gamma$ radiative decay competes with and eventually dominates the $2pnl \rightarrow 1s + e^-$ autoionization. This effect can be modeled theoretically with an optical potential [13]. A complex effective quantum number in the $2pnl$ closed channels, given by $E = E_2 - i\frac{\Gamma_{2p\rightarrow 1s}}{2} - \frac{1}{2\nu^2}$ ($\Gamma_{2p\rightarrow 1s} = 2.425 \times 10^{-7}$ a.u.), is used in the MQDT reduction step of Eq. (2), allowing for radiative decay of the $2p$ core, and resulting in a broadened and reduced, or damped, photoionization cross section in Eq. (3). The redistributed flux contributing to the fluorescence cross section can be computed as [14]

$$\sigma^{\mathrm{fl}} = \frac{4\pi^2\omega}{3c}\,\mathbf{d}_c^{\dagger}(\mathbf{S}^*_{cc} - e^{+i2\pi\nu^*})^{-1}(e^{4\pi\,\mathrm{Im}(\nu)} - 1) \times (\mathbf{S}_{cc} - e^{-i2\pi\nu})^{-1}\mathbf{d}_c\,. \quad (5)$$

Neglecting the nondegeneracy in ν due to the $-i\frac{\Gamma_{2p\rightarrow 1s}}{2}$ term, the expressions in the denominators can be rotated to diagonal form, giving for the fluorescence cross section a sum of noninteracting Lorentzian profiles,

$$\sigma^{\mathrm{fl}} = \sum_{A,n} \frac{\sigma_A}{(n-\mu_A)^3} \frac{\Gamma^f_A/2\pi}{(E - E_{A,n})^2 + (\frac{\Gamma^a_{A,n}+\Gamma^f_A}{2})^2}, \quad (6)$$

where $\sigma_A = \frac{4\pi^2\omega}{3c}\sum_i |\mathbf{O}_{iA}(\mathbf{d}_c)_i|^2$, and $\Gamma^f_A = (O^2_{2pns,A} + O^2_{2pnd,A})\Gamma_{2p\rightarrow 1s}$. Equation (2) of Ref. [6] is the energy integral of this result, $\sum_{A,n}\frac{\sigma_A}{(n-\mu_A)^3}\frac{\Gamma^f_A}{\Gamma^a_{A,n}+\Gamma^f_A}$, except here we have $\Gamma^f_A < \Gamma_{2p\rightarrow 1s}$ due to the admixture of the nonradiating $2snp$ states in each rotated channel A.

The results from an LS-coupled calculation reproduce the trends found in Ref. [6]. Whereas at lower n all three series contribute comparably to the fluorescence cross section, due to the smaller $A = +1$ fluorescence branching ratio $\Gamma^f_A/(\Gamma^a_{A,n} + \Gamma^f_A)$, at higher n, the $A = +1$ series dominates because of its much larger oscillator strength. However, as was seen in Ref. [6], the LS-coupled fluorescence cross section (essentially the $A = +1$ series) fails to describe the observed behavior in the intermediate vicinity of threshold.

Allowing for relativistic effects, total spin is not necessarily conserved, and the five LS-forbidden $\{1s\epsilon p, 2snp, 2pns, 2pnd\}$ ($^3P_1$) and $2pnd$ ($^3D_1$) channels need to be considered. Since the dominant effect of the spin-orbit operator for high-n states is a fine-structure splitting of the $2p_{1/2}$ and $2p_{3/2}$ thresholds, causing the valence nl electrons to propagate away from the atom with different wave numbers, a frame transformation method [11,15,16] is used. Unphysical scattering and dipole matrices are partitioned into LS components and recoupled from an LS to a JK coupling scheme via

$$\mathbf{S}^{JK} = \mathbf{T}^{\mathrm{T}}_{LS,JK}\begin{pmatrix} \mathbf{S}^{(^1P_1)} & 0 & 0 \\ 0 & \mathbf{S}^{(^3P_1)} & 0 \\ 0 & 0 & \mathbf{S}^{(^3D_1)} \end{pmatrix}\mathbf{T}_{LS,JK},$$
$$\mathbf{d}^{JK} = \mathbf{T}^{\mathrm{T}}_{LS,JK}\begin{pmatrix} \mathbf{d}^{(^1P_1)} \\ \mathbf{d}^{(^3P_1)} \\ \mathbf{d}^{(^3D_1)} \end{pmatrix} = \mathbf{T}^{\mathrm{T}}_{LS,JK}\begin{pmatrix} \mathbf{d}^{(^1P_1)} \\ \mathbf{0} \\ \mathbf{0} \end{pmatrix}, \quad (7)$$

where $\mathbf{T}_{LS,JK}$ is the orthogonal recoupling transformation matrix [17]. The transformed dipole matrix $\mathbf{d}^{JK}$, when used in the MQDT reduction step of Eq. (2) to obtain the photoionization and fluorescence cross sections in Eqs. (3) and (5), reproduces the LS results, so long as the LS $n = 2$ degenerate ionic energies are retained [11]. For example, the $2pns$ (^1P) and $2pns$ (^3P) LS channels are recoupled to the $2p_{1/2}ns$ and $2p_{3/2}ns$ JK channels, but this transformation is unitary, and due to the zero dipole matrix of the ^3P symmetry in Eq. (7), the photoexcited JK bound channels are still just the ^1P linear combination. Matching via Eq. (2) with degenerate LS energies retains this ^1P in-phase character.

The key step in the frame transformation is to use instead the experimental, split ionic energies given in Table I, allowing each JK-coupled valence orbital to propagate in a threshold-adjusted potential [11,15]. The MQDT reduction step in Eq. (2) then yields a perturbed *physical* JK dipole matrix,

$$\mathbf{d}^{JK} = \mathbf{T}^{\mathrm{T}}_{LS,JK}\mathbf{d}^{LS} + \mathbf{S}_{oc}(\mathbf{S}_{cc} - e^{-i2\pi\nu^{LS}})^{-1}e^{-i2\pi\nu^{JK}} \times (1 - e^{-i2\pi[\nu^{LS}-\nu^{JK}]})\,(\mathbf{S}_{cc} - e^{-i2\pi\nu^{JK}})^{-1}\mathbf{d}^{JK}_c. \quad (8)$$

Here ν^{JK} is determined using the experimental thresholds in Table I, whereas ν^{LS} is determined using only the $2p_{1/2}$

TABLE I. Energies of the lowest He and He^+ states.

Level	Energy (a.u.)	$\hbar\omega$ (eV)
$1s^2$	−0.903 570 39	0.000 000 0
$1s_{1/2}$	0.000 000 00	24.587 595 4
$2p_{1/2}$	1.499 851 29	65.400 947 8
$2s_{1/2}$	1.499 853 42	65.401 005 9
$2p_{3/2}$	1.499 877 98	65.401 674 0

energy. This form clearly shows that when the difference $\Delta\nu = \nu^{LS} - \nu^{JK}$ is an integer, such as far below threshold, where $\Delta\nu \approx 0$, or at 65.389 eV, where $\Delta\nu = 1$, there is no departure from LS predictions. At these energies, the perturbation term in Eq. (8) is zero. More intuitively, at 65.389 eV, for instance, a $2p_{1/2}nl$ outgoing wave acquires an extra half wave as it is propagated away from the atom to its turning point, and another half wave as it is propagated back in, so it is back in phase with the $2p_{3/2}nl$ wave, and there is no interference between the two.

When $\Delta\nu$ is half-integer, on the other hand, such as at 65.382 eV, where $\Delta\nu = 1/2$, the magnitude of the spin-orbit perturbation is maximum, and the greatest departure from LS-coupling predictions is expected. Intuitively, the different outgoing orbitals are π radians out of phase once they have propagated out from the atom and back to the matching radius, so maximum destructive interference occurs between channels. As a result, the *unphysical* inner-region dipole matrix, which has only ^1P character, is reduced, via Eq. (2), to a *physical* inner-region dipole matrix with ^3P and ^3D character as well.

The oscillatory behavior can be seen more quantitatively by comparing actual LS and JK results, shown in Fig. 1 near threshold. Whereas the LS results consist of essentially the $A = +1$ series of slowly descending height, with smaller contributions from the $A = -1$ and $A = 0$ series, the JK results are more complex. The effective quantum numbers differ by one-half at 65.382 eV, and here the JK results show several resonances of nearly equal strength, indicating that there is strong mixing between series (the unconvoluted results show strong signals from all seven JK-allowed members within a Rydberg spacing). At this energy, the $A = +1$ LS series has a fluorescence branching ratio still appreciably less than one, but the JK mixing causes a redistribution of oscillator strength to states with larger fluorescence branching ratios, increasing the overall fluorescence cross section (the classification according to A loses meaning once appreciable mixing occurs). At 65.389 eV, where $\Delta\nu = 1$, the JK results appear almost identical to the LS ones, giving a dip in the energy-averaged cross section. Another rise is seen at 65.392 eV, where $\Delta\nu = 3/2$. This oscillatory mixing behavior continues right up to threshold, but eventually all fluorescence branching ratios approach one and the FY oscillations subside.

We now compare theoretical results to newer experimental ones. The experiment was done at the ARPES end station of the gas phase beam line 6.2L at ELETTRA [18]. Helium was let into a gas cell (pressure of 10^{-2} torr), separated from two multichannel-plate photon detectors by 1000-Å aluminum filters to avoid influence of charged particles and metastable atoms. The detectors were mounted to measure radiation perpendicular to the plane defined by the synchrotron beam and the polarization direction. The monochromator function could be determined by fitting a Voigt function to single peaks with negligible inherent widths. The Lorentzian and Gaussian FWHM were found to be 1.1 meV and 1.3 meV, respectively. This allows us to resolve states of much higher principal quantum numbers than has earlier been observed and to make a detailed investigation of the threshold region. The energy calibration was achieved by assuming a constant quantum defect for the strongest Rydberg series.

Theoretical and experimental FY spectra in the vicinity of threshold are shown in Fig. 2. It is immediately obvious

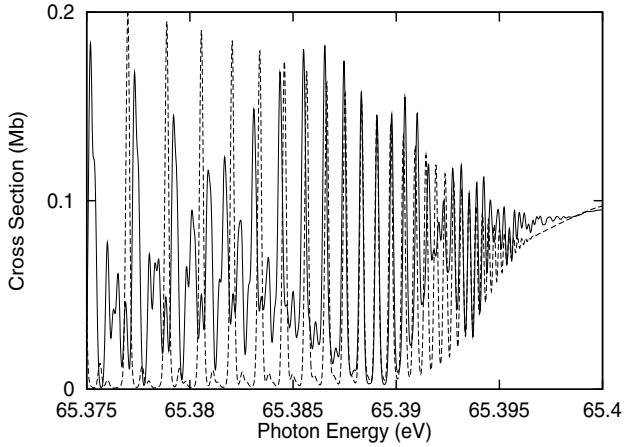

FIG. 1. Comparison of the JK (solid line) and LS (dashed line) fluorescence cross sections, convoluted with a 0.2 meV FWHM Gaussian.

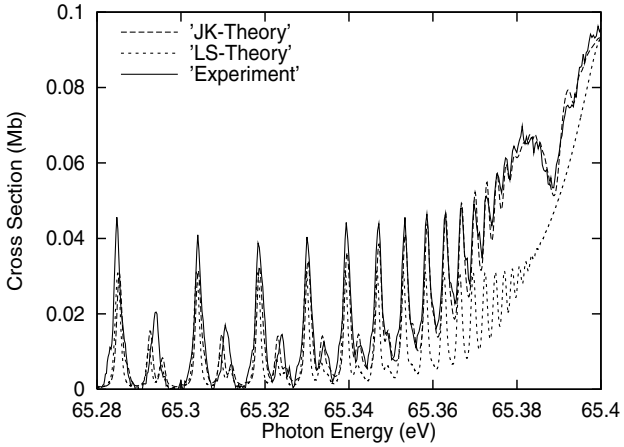

FIG. 2. Helium fluorescence cross sections: theoretical results are convoluted with a Voigt profile; experimental results are arbitrarily normalized to coincide with JK theory near 65.38 eV.

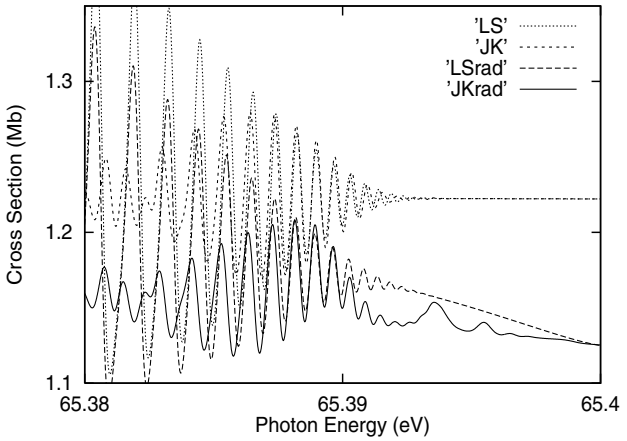

FIG. 3. Theoretical photoionization cross sections near the $n = 2$ threshold of helium, convoluted with 0.5 meV FWHM Gaussians.

that the model based on LS coupling, corresponding to the analysis in Ref. [6], fails to describe the broad peak with maximum at 65.38 eV, and the additional structure closer to threshold. In contrast, the agreement between the experimental results and the relativistic predictions is almost complete. This demonstrates the importance of including relativistic effects in the theoretical description of near-threshold resonance states.

Note that even fine structure in the broad 65.38 eV feature, where $\Delta\nu = 1/2$, is reproduced. Also, a shoulder at 65.392 eV, corresponding to $\Delta\nu = 3/2$ where the second intensity maximum in the oscillations is predicted, can be clearly discerned in the experimental spectrum.

It is also interesting to point out that since fluorescence flux is increased when $\Delta\nu$ is half-integer and decreased again when $\Delta\nu$ is integer, the opposite is expected in the ionization flux—it should decrease when $\Delta\nu$ is half-integer and increase when $\Delta\nu$ is integer. The total photoionization cross section is shown in Fig. 3, and indeed this opposite behavior is seen. Thus, significant ($\approx$10%) radiative damping effects are predicted in the near-threshold ionization yield, with oscillations due to spin-orbit mixing. Indeed, oscillatory behavior just below threshold has recently been observed in new high-resolution measurements at BESSY-II [19].

In conclusion, a combination of R-matrix, MQDT, optical potential, and frame-transformation methods was employed, giving He($2lnl'$) photofluorescence cross sections with LS-forbidden characteristics, reproducing new high-resolution measurements to a remarkable degree. The principal effect of the spin-orbit operator has been quantified as an oscillatory perturbation below threshold, causing strong mixing between different resonance series and redistribution of fluorescence and ionization cross sections at regular intervals. These results should be applicable for highly excited states in general, whenever there are multiple Rydberg series capable of interacting, and emphasize that careful consideration of radiative and relativistic effects is necessary in order to characterize near-threshold photoionization spectra.

T. W. G. thanks F. Robicheaux for valuable discussions. D. D. gratefully acknowledges the support of NSFC. We acknowledge M. De Simone, M. Coreno, and the Machine Group of Elettra for support during the experiment.

*Electronic address: gorczyca@wmich.edu

[1] R. P. Madden and K. Codling, Phys. Rev. Lett. **10**, 516 (1963).
[2] J. W. Cooper, U. Fano, and F. Prats, Phys. Rev. Lett. **10**, 518 (1963).
[3] C. D. Lin, Phys. Rev. A **29**, 1019 (1984).
[4] V. Schmidt, Rep. Prog. Phys. **55**, 1483 (1992).
[5] J. M. Rost, K. Schulz, M. Domke, and G. Kaindl, J. Phys. B **30**, 4663 (1997).
[6] J.-E. Rubensson, C. Såthe, S. Cramm, B. Kessler, S. Stranges, R. Richter, M. Alagia, and M. Coreno, Phys. Rev. Lett. **83**, 947 (1999).
[7] M. K. Odling-Smee, E. Sokell, P. Hammond, and M. A. MacDonald, Phys. Rev. Lett. **84**, 2598 (2000).
[8] K. A. Berrington, W. B. Eissner, and P. H. Norrington, Comput. Phys. Commun. **92**, 290 (1995).
[9] T. W. Gorczyca and N. R. Badnell, J. Phys. B **30**, 3897 (1997).
[10] M. J. Seaton, Rep. Prog. Phys. **46**, 167 (1983).
[11] M. Aymar, C. H. Greene, and E. Luc-Koenig, Rev. Mod. Phys. **68**, 1015 (1996).
[12] J. Yan, Y.-Z. Qu, L. Voky, and J.-M. Li, Phys. Rev. A **57**, 997 (1998).
[13] F. Robicheaux, T. W. Gorczyca, M. S. Pindzola, and N. R. Badnell, Phys. Rev. A **52**, 1319 (1995).
[14] T. W. Gorczyca and F. Robicheaux, Phys. Rev. A **60**, 1216 (1999).
[15] U. Fano, Phys. Rev. A **2**, 353 (1970).
[16] T. W. Gorczyca, Z. Felfli, H.-L. Zhou, and S. T. Manson, Phys. Rev. A **58**, 3661 (1998).
[17] R. D. Cowan, *The Theory of Atomic Structure and Spectra* (University of California, Berkeley, 1981), p. 249.
[18] K. C. Prince, R. R. Blyth, R. Delaunay, M. Zitnik, J. Krempasky, J. Slezak, R. Camilloni, L. Avaldi, M. Coreno, G. Stefani, C. Furlani, M. de Simone, and S. Stranges, J. Synchrotron. Radiat. **5**, 565 (1998).
[19] R. Follath and F. Senf, Synchrotron Radiation News **12**, 34 (1999); W. Gudat (private communication).